



# Molecular displacement approach for the electrochemical detection of protein-bound propofol

David C. Ferrier<sup>\*</sup>, Janice Kiely, Richard Luxton

*Institute of Bio-Sensing Technology, University of the West of England, Frenchay Campus, Bristol BS16 1QY, UK*

## ARTICLE INFO

### Keywords:

Propofol  
Electrochemical sensor  
Nanocomposite  
Albumin  
Protein binding  
Green synthesis

## ABSTRACT

Propofol is one of the principal drugs used for the sedation of patients undergoing mechanical ventilation in intensive care units. The correct dosage of such sedative drugs is highly important, but current methods of determining infusion rates are limited and there is a lack of suitable methods for directly determining patient blood propofol concentrations. A significant challenge for the development of propofol sensors is that propofol demonstrates very high protein binding, leading to a low free fraction in blood. Here we present a method for improving the efficacy of an electrochemical propofol sensor by increasing the free fraction via a molecular displacement approach. When used in conjunction with a carbon nanotube/graphene oxide/iron oxide nanoparticle functionalised screen-printed electrode, it was found that this approach dramatically improved the sensor's sensitivity towards propofol. Ibuprofen was found to be the most effective displacement agent, with an optimal concentration of 30 mM. The resultant sensitivity was 2.82 nA/μg/ml/mm<sup>2</sup> with a coefficient of variation of 0.07, and the limit of detection was 0.2 μg/ml. This approach demonstrates high specificity towards drugs commonly administered to intensive care patients.

## 1. Introduction

Propofol (2,6-diisopropylphenol) is an intravenous anaesthetic used for both anaesthesia and sedation. Due to favourable pharmacokinetic properties, it has been the most commonly used intravenous anaesthetic for the past three decades [1,2], and is one of the most common drugs used to sedate patients undergoing mechanical ventilation in intensive care units (ICUs) [3–6].

The care of patients under mechanical ventilation is challenging and the correct dosage of sedatives such as propofol is highly important. Under-sedation may result in increased patient discomfort as well as immunosuppression and increased blood clotting, whereas over-sedation may result in increased time on ventilation and increased time in the ICU (with the associated demand on resources that ensues) as well as increased risk of brain dysfunction [7–9]. Therefore, the sedation of mechanically ventilated patients needs to be closely monitored.

The most common methods for determining propofol infusion rates involve mathematical models incorporating pharmacokinetic data and patient metrics (such as weight or age). However, these models suffer from poor reliability [10,11]. In addition, propofol pharmacokinetics can vary considerably for ICU patients [3,7], further increasing the

unreliability of these models.

There exists a need for simple and rapid techniques for the determination of a patient's blood propofol concentration. Established laboratory-based techniques such as gas chromatography/mass spectroscopy (GC/MS) and high-performance liquid chromatography (HPLC) suffer from limitations such as high cost, complexity and long reporting times [12]. Several groups have investigated methods of determining blood propofol concentrations via measurement of the concentration in exhaled breath [10,11,13,14]. However, the concentrations of propofol in blood and exhaled breath have been shown to be poorly correlated [15] and respiratory events – such as a reduction in the rate, or cessation, of breathing – can hinder monitoring via breath. Some groups have reported the measurement of propofol and its metabolites in urine [16,17], however, the obvious time-lag makes this approach impractical for patient monitoring.

Direct measurement of propofol in blood presents the most attractive prospect for patient monitoring. However, this presents a specific challenge as it is reported that as little as 2 % of propofol in blood exists free in solution, with the remaining 98 % bound to either erythrocytes or serum proteins [18]. Of the protein bound propofol, some binding will occur to proteins such as α<sub>1</sub>-acid glycoprotein [19,20] and lipoproteins

<sup>\*</sup> Corresponding author.

E-mail address: [david.ferrier@uwe.ac.uk](mailto:david.ferrier@uwe.ac.uk) (D.C. Ferrier).

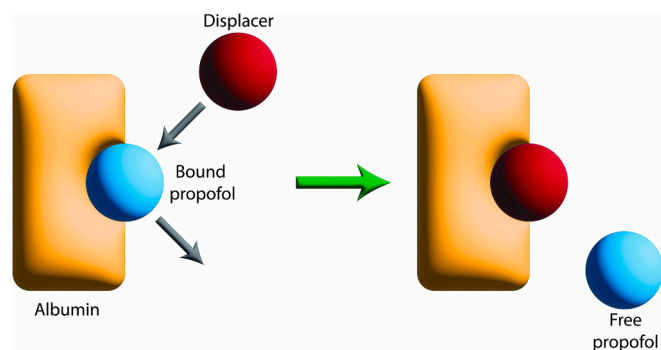


**Fig. 1.** Illustration of the molecular displacement mechanism. The displacer molecule binds preferentially to the same binding site as propofol, therefore displacing propofol and increasing the free propofol concentration.

[20,21], but the majority will be bound to albumin [19,22].

Albumin is the most common serum protein (comprising up to 55 % of all serum proteins [23]) and binds to a wide variety of drugs and other molecules [24–26]. Most drug binding occurs at two particular regions, located on subdomains IIA and IIIA (often referred to as drug binding sites 1 and 2 respectively), although binding does occur at other subdomains. Propofol primarily binds to subdomain IIIA, with a secondary binding site at subdomain IIIB [24,27]. As multiple drugs can compete for the same binding sites of albumin, there is the potential for displacing propofol from its binding sites through competitive binding.

In this paper we present a methodology for improving the efficacy of an electrochemical propofol sensor in serum solutions by introducing a molecular displacer to reduce propofol/albumin binding and increase the propofol free fraction (Fig. 1). This method is paired with a carbon nanotube/graphene oxide/iron oxide nanoparticle (CNT/GO/FeONP) nanocomposite sensor for the simple and rapid detection of propofol in serum samples. In a previous publication we have reported the development of CNT/GO/FeONP nanocomposites for the continuous monitoring of propofol, intended for patients undergoing general anaesthesia [28]. GO enhances the performance of the sensor through its advantageous electrical characteristics and large surface area-to-volume ratio. CNTs act as spacers, preventing the agglomeration of the GO, as well as also possessing favourable electrical characteristics. The FeO nanoparticles act as nanocatalysts for the oxidation reaction, enhancing the sensitivity of the sensor. The metal oxide nanoparticles were synthesised using green synthesis, an emerging field of techniques for the simple and environmentally friendly synthesis of nanomaterials using extracts from plants, bacteria, and fungi. In this work we have investigated discrete detection, intended for use with patients undergoing mechanical ventilation in conjunction with blood samples that are routinely drawn from patients for standard testing, such as blood gas analysis.

## 2. Materials & methods

### 2.1. Materials

Dried bay laurel leaves were purchased from JustIngredients Ltd. (UK). These were rinsed with deionised water and dried prior to use. All other materials were purchased from Merck (Dorset, UK) and used as supplied. Graphene oxide (GO) is 4–10 % edge oxidised (as stated by supplier), and multi-walled carbon nanotubes (CNT) are carboxylic acid functionalised (> 8 %), with an average diameter of 9.5 nm and an average length of 1.5  $\mu\text{m}$  (as stated by supplier).

2,6-diisopropylphenol (97 %) was made up to a 1 mM solution in a 1:9 mixture of dimethyl sulfoxide (DMSO, 99.9 %) and phosphate buffered saline (PBS, 10 mM phosphate buffer, 2.7 mM KCl, 137 mM NaCl, pH 7.4). This solution was then diluted in three different media to produce propofol solutions of concentrations ranging between 0 and 10  $\mu\text{g/ml}$ . The media used were (1) 10 mM PBS, (2) 5 wt% bovine serum

albumin (heat shock fraction, pH 7,  $\geq 98$  %, prepared in 10 mM PBS), and (3) bovine serum (adult).

Similar solutions were prepared using morphine, fentanyl, and midazolam (all from 1 mg/ml stock solutions in methanol) in bovine serum.

Displacer solutions consist of a DMSO solvent containing one of various candidate displacer molecules at concentrations ranging between 50 and 500 mM. The potential displacer molecules investigated were: 8-anilino-1-naphthalene sulfonic acid ammonium salt (ANS,  $\geq 90$  %), ibuprofen, indoxyl sulfate potassium salt, oleic acid (90 %), myristic acid ( $\geq 99$  %) and L-thyroxine ( $\geq 98$  %).

### 2.2. Apparatus

The screen-printed electrodes were purchased from BVT Technologies (Strážek, Czech Republic) and consist of graphite working and counter electrodes and a silver/silver chloride pseudo-reference electrode. The working electrode diameter is 1 mm. All electrochemical measurements were performed using a PalmSens EmStat3 potentiostat.

### 2.3. Sensor functionalisation

The functionalisation of screen-printed electrodes with a CNT/GO/FeONP nanocomposite is described fully in a previous publication [28]. Briefly, a bay leaf extract solution was prepared by grinding 20 g of dried bay leaves to a powder, heating them at 80  $^{\circ}\text{C}$  in 200 ml of deionised water for 10 min and centrifuging to remove any remaining plant material. GO was suspended in 0.1 M  $\text{FeCl}_3$  solution at a concentration of 1 mg/ml and mixed with an equal volume of the bay leaf extract solution. The mixture was left overnight to allow the iron oxide nanoparticles to form. The nanoparticle decorated GO was removed from the solution by centrifugation, mixed with CNT, and re-suspended in deionised water to a concentration of 0.1 mg/ml CNT, 0.05 mg/ml GO. The screen-printed electrode was functionalised by drop-casting the CNT/GO/FeONP nanocomposite solution onto the working electrode using a BioDot AD1520 dispensing system. Five 100 nl droplets were deposited at the centre of the working electrode and allowed to dry at 60 % relative humidity. This procedure was repeated until a total of 1.5  $\mu\text{l}$  of nanocomposite solution had been deposited, then the electrode was rinsed with deionised water and dried in ambient conditions.

### 2.4. Measurement

Prior to electrochemical measurement, 50  $\mu\text{l}$  of bovine serum was deposited onto the sensor surface and cyclic voltammetry performed between  $-0.6$  and  $+0.8$  V at a scan rate of 100 mV/s until a stable baseline was obtained. The electrode is then rinsed with deionised water and dried in air at ambient conditions.

Differential pulse voltammetry (DPV) measurements were performed using a starting potential of  $-0.6$  V, an end potential of  $+0.8$  V, a step potential of 0.02 V, a pulse amplitude of 0.05 V, a pulse duration of 0.2 s, and a scan rate of 50 mV/s. Measurements were performed using 50  $\mu\text{l}$  samples of either 10 mM PBS, 5 wt% BSA (10 mM PBS) or bovine serum with varying propofol concentration.

For displacement experiments, 5  $\mu\text{l}$  of displacer solution were mixed with 45  $\mu\text{l}$  of bovine serum (with a propofol concentration between 0 and 10  $\mu\text{g/ml}$ ), left for 60 s and then deposited on the electrode surface where DPV is performed. After each measurement the electrode surface is rinsed with DI water and dried in ambient conditions. Similar experiments were performed for bovine serum solutions containing morphine, fentanyl or midazolam.

### 2.5. Baseline correction

A custom MatLab algorithm for baseline correction was created, based on that described by Górski et al. [29]. A description of its

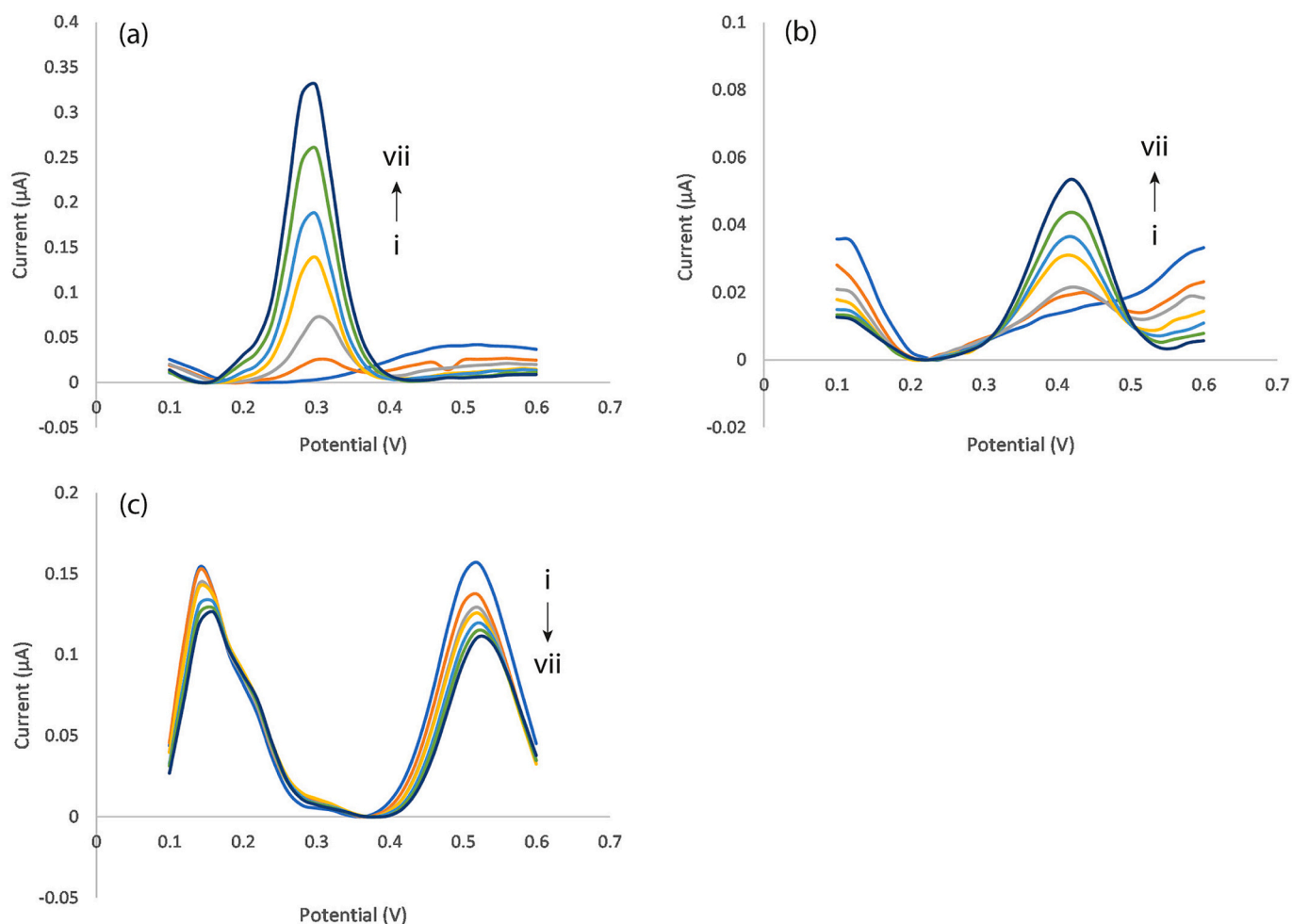


Fig. 2. Differential pulse voltammograms for a) 10 mM phosphate buffered saline (PBS); b) 5 wt% bovine serum albumin, 10 mM PBS; and c) bovine serum solutions with propofol concentrations of (i) 0, (ii) 1, (iii) 2, (iv) 4, (v) 6, (vi) 8, and (vii) 10  $\mu\text{g}/\text{ml}$ .

operation can be found in the Supplementary Information.

### 3. Results & discussion

The optimum polynomial order for baseline correction was found to be fourth-order. Any increase beyond this resulted in negligible improvements in fitting with increased potential for overfitting (i.e. removing signal as well as baseline). Therefore, for all of the DPV results presented in this paper, baseline correction using fourth-order polynomial fitting was performed. Further information is presented in Supplementary Information, Fig. S2.

Figure 2a shows the differential pulse voltammograms for propofol solutions of varying concentrations in 10 mM PBS. A clear, concentration dependant propofol peak can be seen at approximately 300 mV. This peak is caused by the electrochemical oxidation of propofol, which occurs by the same mechanism as other phenolic molecules [30]. Fig. 2b shows the results for the same DPV measurements carried out in a 5 wt% BSA solution (10 mM PBS). While, once again, a clear, concentration dependant propofol peak can be observed, this peak has shifted to approximately 420 mV and the peak currents are significantly reduced (to approximately 20 % of that in PBS). This is the result of a significant proportion of the propofol being bound to the albumin. This albumin concentration is representative of physiological levels [31]. Fig. 2c shows the results for the same DPV measurements carried out in spiked bovine serum. Additional peaks can be seen at approximately 150, 200 and 520 mV which are most likely the result of the presence of dopamine, uric acid [32–36] and amino acids such as L-tyrosine and L-

tryptophan [37–40] all of which would be expected to be present in serum. In the serum case there is no apparent concentration dependant propofol peak, indicating a higher degree of protein binding than is the case for albumin alone. While it is reported that albumin is the major serum protein responsible for propofol binding [18], it is known that other serum proteins bind to propofol, including  $\alpha_1$ -acid glycoprotein [19,20] and lipoproteins [20,21], and this is confirmed by the absence of a propofol peak in Fig. 2c. It is clear from Fig. 2 that a significant majority of propofol is protein bound in serum, and that the free concentration is below the detection limit of these sensors, necessitating a means of increasing the free fraction of propofol.

Indoxyl sulfate, ANS and ibuprofen are all reported to bind to subdomain IIIA of human serum albumin (HSA), each with a binding affinity ( $K_a$ ) two orders of magnitude higher than that of propofol [24,26]. Thyroxine is documented to bind to several binding sites of HSA, including subdomains IIIA and IIIB and to bind to HSA with an affinity one to two orders of magnitude higher than for propofol [24,25,41].

Fatty acids are reported to bind to HSA at seven binding sites, with sites 3 and 4 corresponding to subdomain IIIA and site 5 corresponding to subdomain IIIB [24,42,43]. It has been reported that, when compared to many other fatty acids, oleic acid possesses the highest binding affinity for sites 3, 4 and 5, three orders of magnitude higher than that of propofol [44]. While lower than that of oleic acid, the binding affinity of myristic acid has been reported to be two to three orders of magnitude higher than that of propofol [26,44].

However, indoxyl sulfate, thyroxine and ANS were all found to be electrochemically active in the same potential range as propofol

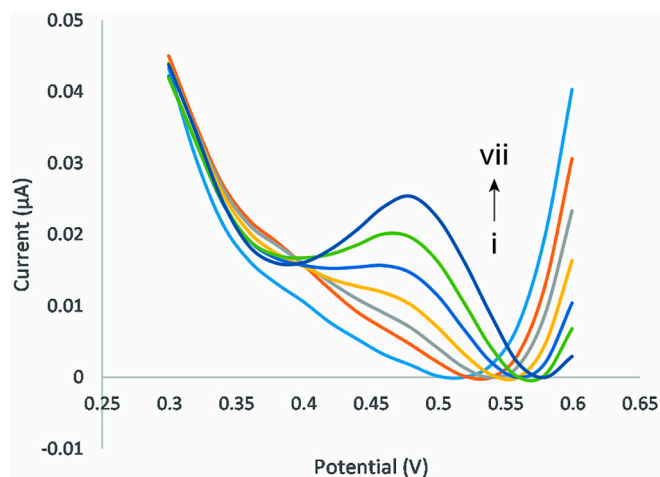


**Fig. 3.** Differential pulse voltammograms of propofol in bovine serum using ibuprofen displacer. Ibuprofen concentration is 30 mM (10 % dimethyl sulfoxide (DMSO)), propofol concentrations are: (i) 0, (ii) 1, (iii) 2, (iv) 4, (v) 6, (vi) 8, and (vii) 10  $\mu\text{g/ml}$ .

(Supplementary Information, Fig. S3) and were discounted as possible displacers for this reason. Ibuprofen has also been reported to be electrochemically active, but at potentials beyond the range investigated here [45–47].

DMSO is used as a solvent for the displacers as it is known to dissolve a wide range of compounds, including hydrophobic molecules [48]. The final concentration in serum is kept to 10 % as it is known that, above this level, it can contribute to protein unfolding [49,50].

Figure 3 shows DPVs performed in bovine serum containing propofol with concentrations spanning the therapeutic range (1–10  $\mu\text{g/ml}$ ) [51] with the addition of ibuprofen (with a final concentration of 30 mM and 10 % DMSO) as a displacer. It can be seen that there is a clear, concentration dependant peak at approximately 480 mV, corresponding to the oxidation of propofol. This peak is absent without the inclusion of the ibuprofen (see Fig. 2c) showing that the ibuprofen is effectively increasing the free fraction of propofol by displacing the albumin bound propofol. This method allows the detection of propofol in serum at concentrations that are not possible without the addition of a displacer.

Figure 4A shows the current at 480 mV against propofol concentration for DPV performed in bovine serum with varying ibuprofen concentration. Fig. 4B shows the resultant gradient for a least-squares linear

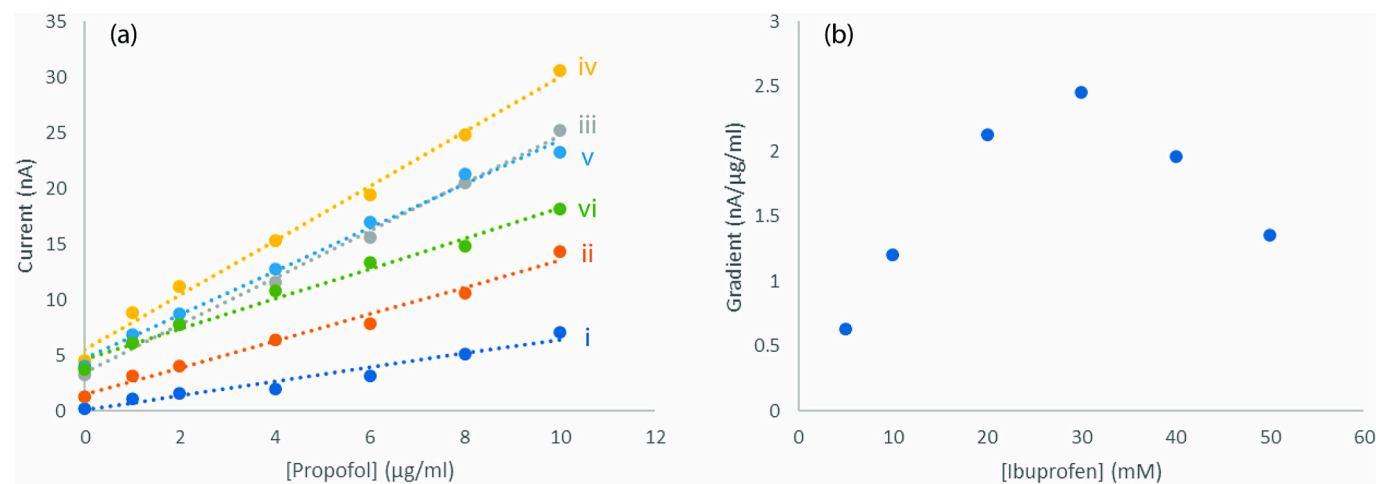


**Fig. 4.** a) Current at 480 mV versus propofol concentration for differential pulse voltammograms in bovine serum. The displacer is ibuprofen at final concentrations of: (i) 5, (ii) 10, (iii) 20, (iv) 30, (v) 40, and (vi) 50 mM. In all cases the DMSO concentration is 10 %. b) The gradient of a least-squares linear fit versus ibuprofen concentration.

fit versus ibuprofen concentration. The sensitivity increases with ibuprofen concentration, indicating a higher free fraction of propofol and therefore a greater degree of displacement, up to 30 mM. Above 30 mM the sensitivity begins to decline, potentially indicating saturation. Additionally, the linearity appears to increase with increasing ibuprofen concentration, but also declines above 30 mM. From this we conclude that a final ibuprofen concentration of 30 mM is optimal for displacing propofol from bovine serum albumin.

Oleic acid and myristic acid were also found to be effective displacers for propofol, however, to a significantly lesser degree than ibuprofen (Supplementary Information, Fig. S4). It is known that fatty acids and drugs bind to albumin in different ways, with fatty acid binding producing global conformational changes, whereas drugs produce only local changes [24]. This difference may account for the different efficacies as molecular displacers. Additionally, albumin site IIIA, the principal binding site for propofol, is also the principal binding site for ibuprofen, whereas this region corresponds to fatty acid binding sites 3 and 4 out of 7 [24]. Therefore, any given molecule of ibuprofen is more likely to occupy the principal binding site of propofol than a given molecule of a fatty acid.

Whilst ibuprofen may be present in a patient's blood as a result of

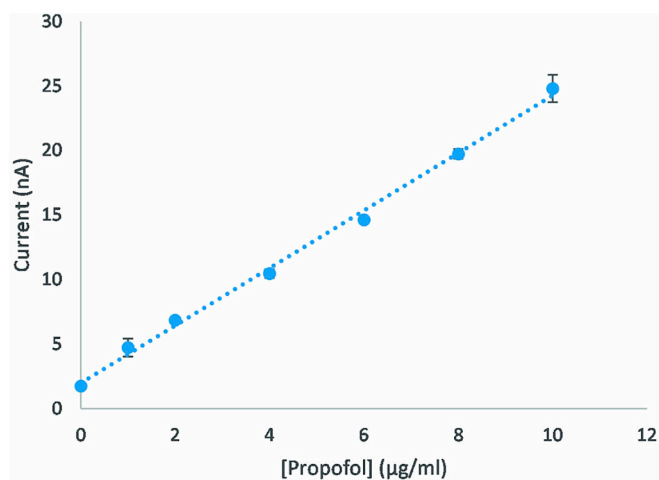


**Fig. 5.** Average current at 480 mV for three electrodes versus propofol concentration in bovine serum. Ibuprofen concentration is 30 mM (10 % DMSO). The error bars represent one standard deviation.

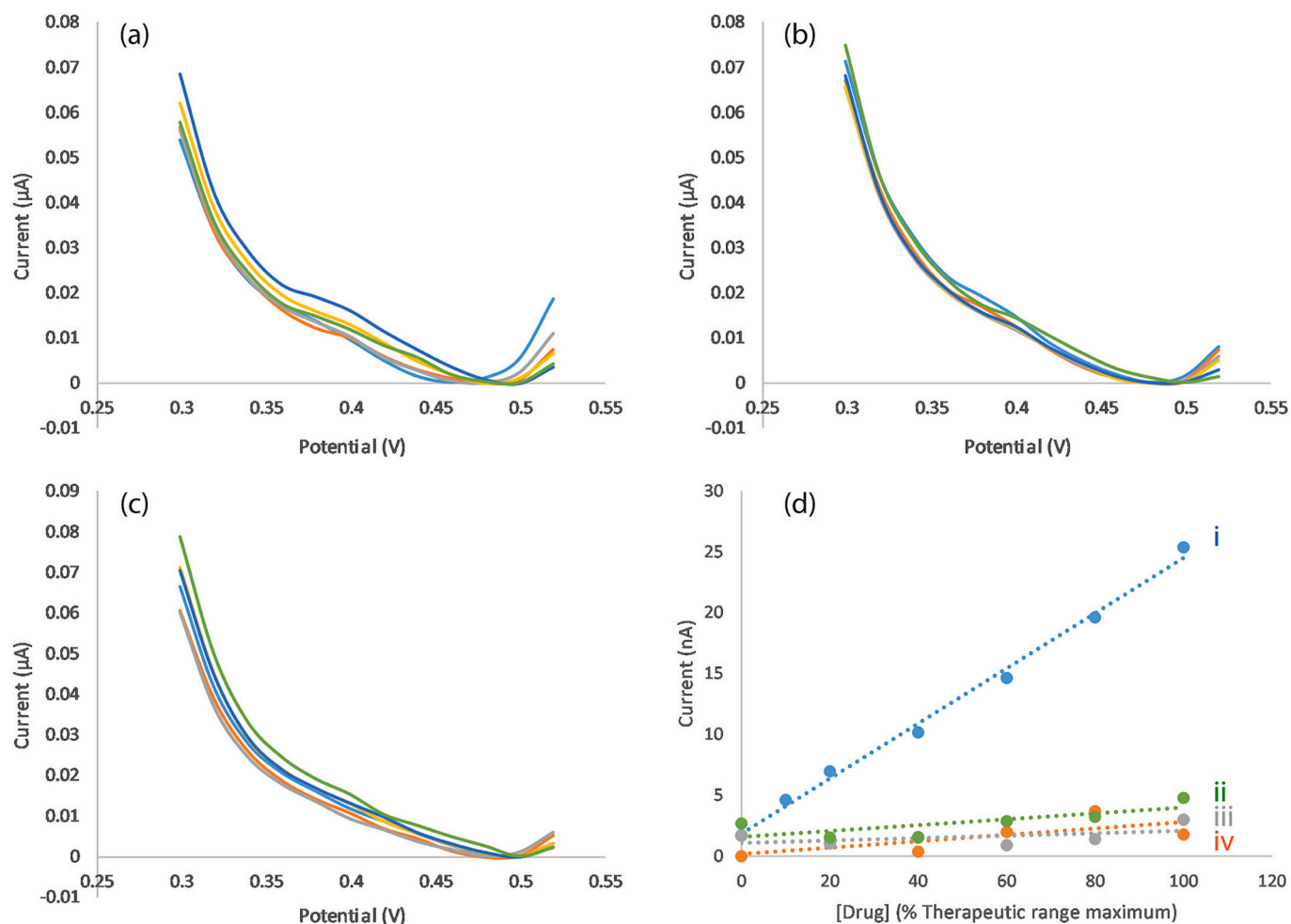


**Fig. 6.** Differential pulse voltammograms of three potential interfering drugs: a) morphine (0–100 ng/ml), b) fentanyl (0–300 ng/ml), c) midazolam (0–100 ng/ml). d) Current at 480 mV versus concentration for each drug and comparison with equivalent for propofol (i) propofol, (ii) midazolam, (iii) fentanyl, (iv) morphine). In all cases medium is bovine serum, 10 % DMSO and 30 mM ibuprofen.

medication, it is unlikely that this would significantly impact the displacement process. The upper end of the therapeutic range for ibuprofen is 30–50 μg/ml [51], which corresponds to less than 1 % of the optimal displacement concentration.

Figure 5 shows the average current versus propofol concentration (for three sensors) for an ibuprofen concentration of 30 mM (10 % DMSO) in bovine serum. There is a clear linear response across the therapeutic range of propofol [51]. The limit of detection (LoD) is 0.2 μg/ml, using the formula:  $LoD = 3.3 \frac{\sigma_{low}}{gradient}$ , where  $\sigma_{low}$  is the standard deviation at a low propofol concentration. The sensitivity is 2.82 nA/μg/ml/mm<sup>2</sup> with a coefficient of variation of 0.07. In the absence of the ibuprofen displacer, this sensor is not capable of detecting propofol at these concentrations in bovine serum (Supplementary information, Fig. S5). Similar experiments were performed for an ibuprofen concentration of 30 mM with mixing times of 30 and 120 s (Supplementary Information, Fig. S6). There is little discernible difference between the current responses for each of these mixing times, indicating that maximal propofol displacement has occurred.

This limit of detection is of a similar magnitude to those of the spectrophotometric approaches for discrete propofol detection described by Gad-Kariem and Abounassif [16] and Liu et al. [52], who report limits of 0.28 μg/ml in plasma and 0.25 μg/ml in whole blood respectively. It is lower than those of the fluorescence approaches reported by Šrámková et al. [53] and Diaó et al. [54] (1.3 and 0.5 μg/ml respectively), but these approaches have only been reported for

application to propofol emulsions.

Figure 6 shows identical DPV measurements performed with varying concentration of three potential interfering compounds. Morphine (Fig. 6a) and fentanyl (Fig. 6b) are two of the most commonly used opioids for pain management in ICU patients [7,9]. Midazolam (Fig. 6c) is a benzodiazepine and is one of the most commonly used sedatives in ICUs [7,9,55]. It can be seen that there are no significant redox peaks within the measurement range and no significant change in current with respect to concentration when compared to propofol (Fig. 6d). In each case, the drug concentration was varied across its therapeutic range (morphine – 0.01 to 0.1 μg/ml; fentanyl – 0.005 to 0.3 μg/ml; midazolam – 0.04 to 0.1 μg/ml [51,56]).

Morphine is known to bind to HSA, with a lower affinity than propofol [57]. However, it has been shown to bind to a location to which neither propofol nor ibuprofen bind, suggesting that it will most likely be unaffected by the presence of the displacer solution. Fentanyl is typically 80–85 % bound to plasma proteins but binds to HSA with a lower affinity than propofol [57,58]. Its primary binding site on HSA is not a binding site for either propofol or ibuprofen, but it has a secondary binding site at site IIIA [57] suggesting that the presence of the displacer solution may result in an increased free fraction of fentanyl, but any increase is likely to be less significant than for propofol. Midazolam is known to bind to HSA at the same location as both propofol and ibuprofen at site IIIA, and to display a binding affinity of the same order of magnitude as propofol [59]. It is therefore likely that the presence of the displacer solution will result in an increased free fraction of

mizazolam. It is clear from Fig. 6 that, irrespective of any potential influence of the displacer upon the protein binding of these potential interfering compounds, the sensor demonstrates high specificity towards them.

#### 4. Concluding remarks

We have demonstrated a method for improving the efficacy of an electrochemical propofol sensor by the molecular displacement of protein-bound propofol, thereby increasing the free fraction. We found that, of those investigated, ibuprofen presents the best candidate as a displacer molecule, producing the highest degree of displacement whilst not being electrochemically active in the same potential region as propofol. The optimal final ibuprofen concentration was found to be 30 mM.

Used in conjunction with a CNT/GO/FeONP nanocomposite functionalised screen-printed electrode sensor, this method results in a linear response across the therapeutic range of propofol with a limit of detection that is superior to that of reported optical-based discrete propofol measurement techniques. This sensor performance is simply not possible without the application of the molecular displacement technique.

This approach is simple, rapid and produces results with a high degree of specificity towards drugs commonly administered to ICU patients. This molecular displacement technique could potentially be applied to the detection of other highly protein-bound molecules. Future work will include investigation of any differences in optimal displacer concentration when applied to human serum albumin and investigation of this technique applied to whole blood, or its incorporation with a suitable plasma separation method.

#### Funding

This work was supported by funding from Somnus Scientific Ltd. The funders had no role in study design, data collection and analysis, or decision to publish.

#### CRedit authorship contribution statement

**David C. Ferrier:** Writing – review & editing, Writing – original draft, Methodology, Investigation, Conceptualization. **Janice Kiely:** Writing – review & editing, Funding acquisition. **Richard Luxton:** Writing – review & editing, Funding acquisition.

#### Declaration of competing interest

The authors declare the following financial interests/personal relationships which may be considered as potential competing interests: David Ferrier has patent #GB2312650.1 pending to Somnus Scientific Ltd.

#### Data availability

Data will be made available on request.

#### Acknowledgements

The authors would like to thank Dr. Kathryn Lamb-Riddell for her help with BioDot programming, as well as Mark O'Connell and Tim Craft of Somnus Scientific Ltd. for their comments and suggestions.

#### Appendix A. Supplementary data

Supplementary data to this article can be found online at <https://doi.org/10.1016/j.sbsr.2024.100710>.

#### References

- [1] F. Kivilehan, E. Chaum, E. Lindner, Propofol detection and quantification in human blood: the proise of feedback controlled, closed-loop anesthesia, *Analyst* 140 (2015) 98–106, <https://doi.org/10.1039/C4AN01483A>.
- [2] M.M. Sahinovic, M.M.R.F. Struys, A.R. Absalom, Clinical pharmacokinetics and pharmacodynamics of propofol, *Clin. Pharmacokinet.* 57 (2018) 1539–1558, <https://doi.org/10.1007/s40262-018-0672-3>.
- [3] J. Barr, T.D. Egan, N.F. Sandoval, K. Zomorodi, C. Cohane, P.L. Gambus, S. L. Shafer, Propofol dosing regimens for ICU sedation based upon and integrated pharmacokinetic-pharmacodynamic model, *Anesthesiol* 95 (2001) 324–333, <https://doi.org/10.1097/0000542-200108000-00011>.
- [4] J. Barr, G.L. Fraser, K. Puntillo, et al., Clinical practice guidelines for the management of pain, agitation, and delirium in adult patients in the intensive care unit, *Crit. Care Med.* 41 (2013) 263–306, <https://doi.org/10.1097/CCM.0b013e3182783b72>.
- [5] J.W. Devlin, Y. Skrobik, C. Gélinas, et al., Clinical practice guidelines for the prevention and management of pain, agitation/sedation, delirium, immobility, and sleep disruption in adult patients in the ICU, *Crit. Care Med.* 46 (2018) e825–e873, <https://doi.org/10.1097/CCM.0000000000003299>.
- [6] K. Yamamoto, Risk of propofol use for sedation in COVID-19 patients, *Anaesthesiol. Intensive Ther.* 52 (2020) 354–355, <https://doi.org/10.5114/ait.2020.100477>.
- [7] C.G. Hughes, S. McGrane, P.P. Pandharipande, Sedation in the intensive care setting, *Clin. Pharmacol.: Adv. Appl.* 4 (2021) 53–63, <https://doi.org/10.2147/CPAA.S26582>.
- [8] R.J. Nies, C. Muller, R. Pfister, P.S. Binder, N. Nosseir, F.S. Nettersheim, K. Kuhr, M. H.J. Wiesen, M. Kochanek, G. Michels, Monitoring of sedation depth in intensive care unit by therapeutic drug monitoring? A prospective observation study of medical intensive care patients, *J. Intensive Care* 6 (2018) 62, <https://doi.org/10.1186/s40560-018-0331-7>.
- [9] K. Rowe, S. Fletcher, Sedation in the intensive care unit, *Contin. Educ. Anaesth. Crit. Care Pain* 8 (2008) 50–55, <https://doi.org/10.1093/bjaceacp/mkn005>.
- [10] T. Laurila, T. Sorajärvi, J. Saarela, J. Toivonen, D.W. Wheeler, L. Ciffioni, G.A. D. Ritchie, C.F. Kaminski, Optical detection of the anesthetic agent propofol in the gas phase, *Anal. Chem.* 83 (2011) 3963–3967, <https://doi.org/10.1021/ac200690f>.
- [11] F. Zhang, H. Dong, X. Zhang, J. Guo, Y. Liu, C. Zhou, X. Zhang, J. Liu, M. Yan, X. Chen, A non-invasive monitoring of propofol concentration in blood by a virtual surface acoustic wave sensor array, *Anal. Sci.* 33 (2017) 1271–1277, <https://doi.org/10.2116/analsci.33.1271>.
- [12] D.C. Ferrier, J. Kiely, R. Luxton, Propofol detection for monitoring of intravenous anaesthesia: a review, *J. Clin. Monit. Comput.* 36 (2022) 315–323, <https://doi.org/10.1007/s10877-021-00738-5>.
- [13] C. Hornuss, S. Praun, J. Villinger, A. Dornauer, P. Moehnle, D.M.E. Weniger, A. Chouker, C. Feil, J. Briegel, M. Thiel, G. Schelling, Real-time monitoring of propofol in expired air in humans undergoing total intravenous anesthesia, *Anesthesiol* 106 (2007) 665–674, <https://doi.org/10.1097/01.anes.0000264746.01393.e0>.
- [14] T. Perl, E. Carstens, A. Hirn, M. Quintel, M. Vautz, J. Nolte, M. Jünger, Determination of serum propofol concentrations by breath analysis using ion mobility spectrometry, *Br. J. Anaesth.* 103 (2009) 822–827, <https://doi.org/10.1093/bja/aep312>.
- [15] W. Miekisch, P. Fuchs, S. Kamysek, C. Neumann, J.K. Schubert, Assessment of propofol concentrations in human breath and blood by means of HS-SPME-GC-MS, *Clin. Chimica Acta.* 395 (2008) 32–37, <https://doi.org/10.1016/j.cca.2008.04.021>.
- [16] E.A. Gad-Kariem, M.A. Abounassif, Colorimetric determination of propofol in bulk form, dosage form and biological fluids, *Anal. Lett.* 33 (2000) 2515–2531, <https://doi.org/10.1080/00032710008543206>.
- [17] S.Y. Lee, N.-H. Park, E.-K. Jeong, J.-W. Wi, C.-J. Kim, J.Y. Kim, M.K. In, J. Hong, Comparison of GC/MS and LC/MS methods for the analysis of propofol and its metabolites in urine, *J. Chromatogr. B* 900 (2012) 1–10, <https://doi.org/10.1016/j.jchromb.2012.05.011>.
- [18] J.X. Mazoit, K. Samii, Binding of propofol to blood components: implications for pharmacokinetics and for pharmacodynamics, *Br. J. Clin. Pharmacol.* 47 (1999) 35–42, <https://doi.org/10.1046/j.1365-2125.1999.00860.x>.
- [19] Z. Sun, H. Xu, Y. Cao, F. Wang, W. Mi, Elucidating the interaction of propofol and serum albumin by spectroscopic and docking methods, *J. Mol. Liq.* 219 (2016) 405–410, <https://doi.org/10.1016/j.molliq.2016.03.040>.
- [20] M.K. Zamacona, E. Suarez, E. Garcia, C. Aguirre, R. Calvo, The significance of lipoproteins in serum binding variations of propofol, *Anesth. Analg.* 87 (1998) 1147–1151, <https://doi.org/10.1213/0000539-199811000-00032>.
- [21] O. Bandschapp, C. Chenaud, I. Inan, B. Walder, P. Merlani, A. Weber, P. Roux-Lombard, B. Ricou, Propofol and perioperative inflammation—the intralipid solvent may play a role, *Glob. Anesth. Perioper. Med.* 1 (2015) 96–103, <https://doi.org/10.15761/GAPM.1000124>.
- [22] A.A. Bhattacharya, S. Curry, N.P. Franks, Binding of the general anesthetics propofol and halothane to human serum albumin, *J. Biol. Chem.* 275 (2000) 38731–38738, <https://doi.org/10.1074/jbc.M005460200>.
- [23] M.P. Czub, K.B. Handing, B.S. Venkataramany, D.R. Cooper, I.G. Shabalin, W. Minor, Albumin-based transport of nonsteroidal anti-inflammatory drugs in mammalian blood plasma, *J. Med. Chem.* 63 (2020) 6847–6862, <https://doi.org/10.1021/acs.jmedchem.0c00225>.
- [24] J. Ghuman, P.A. Zunsain, I. Petitpas, A.A. Bhattacharya, M. Otagiri, S. Curry, Structural basis on the drug-binding specificity of human serum albumin, *J. Mol. Biol.* 353 (2005) 38–52, <https://doi.org/10.1016/j.jmb.2005.07.075>.

- [25] A. Varshney, P. Sen, E.R.M. Ahmad, N. Subbarao, R.H. Khan, Ligand binding strategies of human serum albumin: how can the cargo be utilized? *Chirality* 22 (2010) 77–87, <https://doi.org/10.1002/chir.20709>.
- [26] F. Zsila, Subdomain IB is the third major drug binding region of human serum albumin: toward the three-sites model, *Mol. Pharm.* 10 (2013) 1668–1682, <https://doi.org/10.1021/mp400027q>.
- [27] M. Fasano, S. Curry, E. Terreno, M. Galliano, G. Fanali, P. Narciso, S. Notari, P. Ascenzi, The extraordinary ligand binding properties of human serum albumin, *IUBMB Life* 57 (2005) 787–796, <https://doi.org/10.1080/15216540500404093>.
- [28] D.C. Ferrier, J. Kiely, R. Luxton, Metal oxide decorated carbon nanocomposite electrodes for propofol monitoring, *Biosens. Bioelectron.* X 12 (2022) 100286, <https://doi.org/10.1016/j.biosx.2022.100286>.
- [29] L. Górski, F. Ciepela, M. Jakubowska, Automatic baseline correction in voltammetry, *Electrochim. Acta* 136 (2014) 195–203, <https://doi.org/10.1016/j.electacta.2014.05.076>.
- [30] M. Ferreira, H. Varela, R.M. Torresil, G. Tremmiliosi-Filho, Electrode passivation caused by polymerization of different phenolic compounds, *Electrochim. Acta* 52 (2006) 434–442, <https://doi.org/10.1016/j.electacta.2006.05.025>.
- [31] J.W. Kim, M.S. Byun, J.H. Lee, D. Yi, S.Y. Jeon, B.K. Sohn, J.-Y. Lee, S.A. Shin, Y. K. Kim, K.M. Kang, C.-H. Sohn, D.Y. Lee, Serum albumin and beta-amyloid deposition in the human brain, *Neuro* 95 (2020) e815–e826, <https://doi.org/10.1212/WNL.00000000000010005>.
- [32] M. Ben Atyah, L. Bounab, M. Choukairi, R. El Khamlichi, D. Bouchta, F. Chaouket, I. Raissouni, Selective and sensitive detection of dopamine in the presence of ascorbic acid and uric acid at a sonogel-carbon L-histidine modified electrode, *J. Mater. Environ. Sci.* 9 (2018) 66–76, <https://doi.org/10.26872/j.jmes.2018.9.1.8>.
- [33] M. Choukairi, D. Bouchta, L. Bounab, M. Ben Atyah, R. Elkhmalichi, F. Chaouket, I. Raissouni, I.N. Rodriguez, Electrochemical detection of uric acid and ascorbic acid: application in serum, *J. Electroanal. Chem.* 758 (2015) 117–124, <https://doi.org/10.1016/j.jelechem.2015.10.012>.
- [34] M. Kundys-Siedlecka, E. Baczynska, M. Jonsson-Niedziolka, Electrochemical detection of dopamine and serotonin in the presence of interferences in a rotating droplet system, *Anal. Chem.* 91 (2019) 10908–10913, <https://doi.org/10.1021/acs.analchem.9b02967>.
- [35] N. Murugan, M.B. Chan-Park, A.K. Sundramoorthy, Electrochemical detection of uric acid on exfoliated nanosheets of grahitic-like carbon nitride (g-C<sub>3</sub>N<sub>4</sub>) based sensor, *J. Electrochem. Soc.* 166 (2019) B3163–B3170, <https://doi.org/10.1149/2.0261909jes>.
- [36] A. Üge, D.K. Zeybeck, B. Zeybeck, An electrochemical sensor for sensitive detection of dopamine based on MWCNTs/CeO<sub>2</sub>-PEDOT composite, *J. Electroanal. Chem.* 813 (2018) 134–142, <https://doi.org/10.1016/j.jelechem.2018.02.028>.
- [37] H. Cheng, C. Chen, S. Zhang, Electrochemical behaviour and sensitive determination of L-tyrosine with a gold nanoparticles modified glassy carbon electrode, *Anal. Sci.* 25 (2009) 1221–1225, <https://doi.org/10.2116/analsci.25.1221>.
- [38] C. Kavitha, K. Bramhaiah, N.S. John, Low-cost electrochemical detection of L-tyrosine using an rGO-cu modified pencil graphite electrode and its surface orientation on a ag electrode using an ex situ spectroelectrochemical method, *RSC Adv.* 10 (2020) 22871–22880, <https://doi.org/10.1039/d0ra04015k>.
- [39] F. Pogacean, C. Varodi, M. Coros, I. Kacso, T. Radu, B.I. Cozar, V. Mirel, S. Pruneanu, Investigation of L-tryptophan electrochemical oxidation with a graphene-modified electrode, *Biosens* 11 (2021) 36, <https://doi.org/10.3390/bios11020036>.
- [40] Z.Z. Tasić, M.B.P. Mihajlović, M.B. Radovanović, A.T. Simonović, D.V. Medić, M. M. Antonijević, Electrochemical determination of L-tryptophan in food samples on graphite electrode prepared from waste batteries, *Sci. Rep.* 12 (2022) 5469, <https://doi.org/10.1038/s41598-022-09472-7>.
- [41] I. Petitpas, C.E. Petersen, C.-E. Ha, A.A. Bhattacharya, P.A. Zunszain, J. Ghuman, N.V. Bhagavan, S. Curry, Structural basis of albumin-thyroxine interactions and familial dysalbuminemic hyperthyroxinemia, *Proc. Natl. Acad. Sci.* 100 (2003) 6440–6445, <https://doi.org/10.1073/pnas.1137188100>.
- [42] S. Fujiwara, T. Amisaki, Fatty acid binding to serum albumin: molecular simulation approaches, *Biochim. Biophys. Acta* 2013 (1830) 5427–5434, <https://doi.org/10.1016/j.bbagen.2013.03.032>.
- [43] E.S. Krenzel, Z. Chen, J.A. Hamilton, Correspondence of fatty acid and drug binding sites on human serum albumin: a two dimensional nuclear magnetic resonance study, *Biochem* 52 (2013) 1559–1567, <https://doi.org/10.1021/bi301458b>.
- [44] A.A. Spector, Fatty acid binding in plasma albumin, *J. Lipid Res.* 16 (1975) 165–179, [https://doi.org/10.1016/S0022-2275\(20\)36723-7](https://doi.org/10.1016/S0022-2275(20)36723-7).
- [45] S. Amin, M.T. Soomro, N. Memon, A.R. Solangi, T. Sirajuddin, A.R. Behzad Quershi, Disposable screen printed graphite electrode for the direct electrochemical determination of ibuprofen in surface water, *Environ. Nanotechnol., Monit. Manag.* 1–2 (2014) 8–13, <https://doi.org/10.1016/j.enmm.2014.07.001>.
- [46] B. Mekassa, M. Tessema, B.S. Chandravanshi, M. Tefera, Square wave voltammetric determination of ibuprofen at poly(L-aspartic acid) modified glassy carbon electrode, *IEEE Sensors J.* 18 (2018) 37–44, <https://doi.org/10.1109/JSEN.2017.2769137>.
- [47] N. Serrano, O. Castilla, C. Ariño, M.S. Diaz-Cruz, J.M. Díaz-Cruz, Commercial screen-printed electrodes based on carbon nanomaterials for a fast and cost-effective voltammetric determination of paracetamol, ibuprofen and caffeine in water samples, *Sens* 19 (2019) 4039, <https://doi.org/10.3390/s19184039>.
- [48] C. Senac, S. Desgranges, C. Contino-Pépin, W. Urbach, P.F.J. Fuchs, N. Taulier, Effect of dimethyl sulfoxide on the binding of 1-adamantane carboxylic acid to  $\beta$ - and  $\gamma$ -cyclodextrins, *ACS Omega* 3 (2018) 1014–1021, <https://doi.org/10.1021/acsomega.7b01212>.
- [49] T. Arakawa, Y. Kita, S.N. Timasheff, Protein precipitation and denaturation by dimethyl sulfoxide, *Biophys. Chem.* 131 (2007) 62–70, <https://doi.org/10.1016/j.bpc.2007.09.004>.
- [50] A.N.L. Batista, J.M. Batista, V.S. Bolzani, M. Furlan, E.W. Blanch, Selective DMSO-induced conformational changes in proteins from Raman optical activity, *Phys. Chem. Chem. Phys.* 15 (2013) 20147, <https://doi.org/10.1039/C3CP53525H>.
- [51] R. Regenthal, M. Krueger, C. Koepfel, R. Preiss, Drug levels: therapeutic and toxic serum/plasma concentrations of common drugs, *J. Clin. Monit.* 15 (1999) 529–544, <https://doi.org/10.1023/a:1009935116877>.
- [52] B. Liu, D.M. Pettigrew, S. Bates, P.G. Laitenberger, G. Troughton, Performance evaluation of a whole blood propofol sensor, *J. Clin. Monit. Comput.* 26 (2012) 29–36, <https://doi.org/10.1007/s10877-011-9330-0>.
- [53] I. Šrámková, C.G. Amorim, H. Sklenářová, M.C.B.M. Montenegro, B. Horstkotte, A. N. Araújo, P. Solich, Fully automated analytical procedure for propofol determination by sequential injection technique with spectrophotometric and fluorimetric detections, *Talanta* 118 (2014) 104–110, <https://doi.org/10.1016/j.talanta.2013.09.059>.
- [54] J. Diao, T. Wang, L. Li, Graphene quantum dots as nanoprobe for fluorescent detection of propofol in emulsions, *R. Soc. Open Sci.* 6 (2019) 181753, <https://doi.org/10.1098/rsos.181753>.
- [55] S.D. Pearson, B.K. Patel, Evolving targets for sedation during mechanical ventilation, *Curr. Opin. Crit. Care* 26 (2020) 47–52, <https://doi.org/10.1097/MCC.0000000000000687>.
- [56] M. Schulz, A. Schmoltdt, H. Andresen-Streichert, S. Iwersen-Bergmann, Revisited: therapeutic and toxic blood concentrations of more than 1100 drugs and other xenobiotics, *Crit. Care* 24 (2020) 195, <https://doi.org/10.1186/s13054-020-02915-5>.
- [57] R. Zhou, J.M. Perez-Aguilar, Q. Meng, J.G. Saven, R. Liu, Opioid binding sites in human serum albumin, *Anesth. Analg.* 114 (2012) 122–128, <https://doi.org/10.1213/ANE.0b013e318232e922>.
- [58] S.R. Bista, A. Haywood, J. Hardy, M. Lobb, A. Tapuni, R. Norris, Protein binding of fentanyl and its metabolite nor-fentanyl in human plasma, albumin, and  $\alpha$ -1 acid glycoprotein, *Xenobiotica* 45 (2015) 207–212, <https://doi.org/10.3109/00498254.2014.971093>.
- [59] S.N. Khan, B. Islam, A.U. Khan, Probing midazolam interaction with human serum albumin and its effect on structural state of protein, *Int. J. Integr. Biol.* 1 (2007) 102–112, <https://doi.org/10.1007/s10847-020-01016-8>.